Passive Control of Limit Cycle Oscillations in a Thermoacoustic System using Asymmetry

Bryan Eisenhower * Gregory Hagen † Andrzej Banaszuk ‡ Igor Mezić §

September 5, 2006

Abstract

In this paper we investigate oscillations of a dynamical system containing passive dynamics driven by a positive feedback and how spatial characteristics (i.e. symmetry) affect the amplitude and stability of its nominal limit cycling response. The physical motivation of this problem is thermoacoustic dynamics in a gas turbine combustor. The spatial domain is periodic (passive annular acoustics) which are driven by heat released from a combustion process, and with sufficient driving through this nonlinear feedback a limit cycle is produced which is exhibited by a traveling acoustic wave around this annulus. We show that this response can be controlled *passively* by spatial perturbation in the symmetry of acoustic parameters. We find the critical parameter values that affect this oscillation, study the bifurcation properties, and subsequently use harmonic balance and temporal averaging to characterize periodic solutions and their stability. In all of these cases, we carry a parameter associated with the spatial symmetry of the acoustics and investigate how this symmetry affects the system response. The contribution of this paper is a unique analysis of a particular physical phenomena, as well as illustrating the equivalence of different nonlinear analysis tools for this analysis.

1 Introduction

Thermoacoustic instabilities in gas turbines develop when acoustics in a combustor couple with an unsteady heat-release in a positive feedback loop. Thermoacoustic modeling and control is well-studied for axially extended combustion chambers, as in [1, 2, 3, 4], where the acoustic to heat-release coupling is dominated by longitudinal acoustic modes. Because different instability regimes occur at different operating conditions, recent attention has focussed on thermoacoustic modeling in combustion chambers with annular, or cylindrical geometries [5, 6, 7, 8, 9].

Control of thermoacoustic oscillations is a rich field due to the complexity of the dynamics as well as the prominence of both land and air-based jet engines. These high-energy devices operate in a wide range of operating conditions, all of which are highly nonlinear due to turbulence, combustion, and other extreme conditions. The oscillations lead to compromised performance, high noise levels, or catastrophic engine damage. Current control means (see [10]) include avoiding operating conditions which exhibit large oscillations, additional dissipation including acoustic dampers or resonators [11], or in some cases active feedback control [12, 13, 14]. The first option is detrimental in terms of marketing/engine use while redesign using dampers and resonators takes time and adds weight. Active control is challenging due to actuator limitations including harsh conditions, high temporal frequencies, and the limited amount of control authority a finite number of actuators offers.

With these limitations in mind, any approach that opens the operating envelope, and does not add weight or significant complexity and redesign is a valuable solution. In this paper we study

*Student, Department of Mechanical and Environmental Engineering, University of California, Santa Barbara, CA
†Senior Researcher, United Technologies Research Center, 411 Silver Lane, East Hartford, CT 06108
‡Fellow, United Technologies Research Center, 411 Silver Lane, East Hartford, CT 06108
§Professor, Department of Mechanical and Environmental Engineering, University of California, Santa Barbara, CA

Report Documentation Page

Form Approved
OMB No. 0704-0188

1. REPORT DATE	2. REPORT TYPE	3. DATES COVERED
2006		**00-00-2006 to 00-00-2006**

4. TITLE AND SUBTITLE	5a. CONTRACT NUMBER
Passive Control of Limit Cycle Oscillations in a Thermoacoustic System using Asymmetry	5b. GRANT NUMBER
	5c. PROGRAM ELEMENT NUMBER
6. AUTHOR(S)	5d. PROJECT NUMBER
	5e. TASK NUMBER
	5f. WORK UNIT NUMBER
7. PERFORMING ORGANIZATION NAME(S) AND ADDRESS(ES) **Department of Electrical and Computer Engineering,University of California,Santa Barbara,CA,93106**	8. PERFORMING ORGANIZATION REPORT NUMBER
9. SPONSORING/MONITORING AGENCY NAME(S) AND ADDRESS(ES)	10. SPONSOR/MONITOR'S ACRONYM(S)
	11. SPONSOR/MONITOR'S REPORT NUMBER(S)

12. DISTRIBUTION/AVAILABILITY STATEMENT
Approved for public release; distribution unlimited

13. SUPPLEMENTARY NOTES
The original document contains color images.

14. ABSTRACT

15. SUBJECT TERMS

16. SECURITY CLASSIFICATION OF:			17. LIMITATION OF ABSTRACT	18. NUMBER OF PAGES	19a. NAME OF RESPONSIBLE PERSON
a. REPORT	b. ABSTRACT	c. THIS PAGE			
unclassified	**unclassified**	**unclassified**		**14**	

such a solution; introducing precise spatial variations (asymmetry) in a specific mean property of the dynamics which directly affects the amplitude of limit cycle oscillations.

Approaches to analyze thermoacoustic oscillations are abundant, ranging from complex CFD simulation to reduced order analysis. The reduced order analysis often includes spatial approximation of the first principle dynamics resulting in a system of ordinary differential equations. This spatial approximation can be performed many ways including an *element wise* approach or by a modal decomposition. If a modal approach is used, the model is often of very low order (since the thermoacoustic instability is typically tied predominantly to one or two acoustic modes) while the element approach is used, the ODE system will result in numerous coupled oscillators. We mention this here because although our approximation in this study is modal, resulting in two coupled modes (oscillators), the tools used here align with those used in to study synchronized aspects of multiple coupled oscillators.

Interaction of nonlinear oscillator populations has been a rich topic for hundreds of years. From pendulum clock synchronization, to fire-fly flashing, to the interaction of spiking neural activity, the study of the behavior of these systems continues to offer insight into either amplification or control of synchronized behavior in interconnected complex systems. In [15] coupled oscillators in a ring using uniform distribution of natural frequencies were analyzed seeking stable conditions including synchrony and *oscillator death*. Our work seeks similar information while the natural frequencies (acoustic wavespeed) of the oscillator population are perturbed by a spatial pattern instead of a statistical distribution. Similarly traveling wave solutions for a ring of nonlinear oscillators was investigated in [16] while a completely different form of network connection was investigated in [17].

This study differs from typical synchronization studies predominately because we investigate a modal response of the oscillators instead of seeking conditions on n individual oscillators. In addition, most synchronization studies investigate the behavior of oscillators which are self excited in their uncoupled state while here, the coupling itself motivates a limit cycle. Finally, most often synchronization studies investigate binary dynamics that exhibit either on-off or integrate-and-fire responses while with our system different amplitude solutions are prevalent (phase only representations do not suffice). Aside from these differences, the methods used here align significantly with those used in the aforementioned efforts.

The organization of this paper is as follows; we begin by developing a reduced model of the dynamics starting with first principles. The equilibrium of this model is then investigated using numerical bifurcation analysis tools. Following this, the periodic equilibriuma are determined using two methods; Averaging, and Harmonic Balance. The results of these two methods are compared and the limit cycle properties are investigated using both approaches illustrating that altering the symmetry in a specific parameter always reduces the limit cycle amplitude and eventually stabilizes the system. It is also shown that the oscillations during this imposed asymmetry remain stable.

2 Modelling

In this section we briefly describe the thermoacoustic model used in the current analysis. In an annular combustion system, flow passes down the length of an annulus, and is eventually mixed with fuel. When this mixture reaches a series of flames distributed around this annulus, it reacts/combusts. This combustion process both reacts to the acoustics (i.e how the acoustics bring the fuel mixture to the flame), while at the same time it drives the acoustics with its heat release. Figure 1, presents a schematic of the annular combustor and feedback interconnection between the acoustics and heat release.

The fundamental structure and justification of all assumptions of the transport equations for this

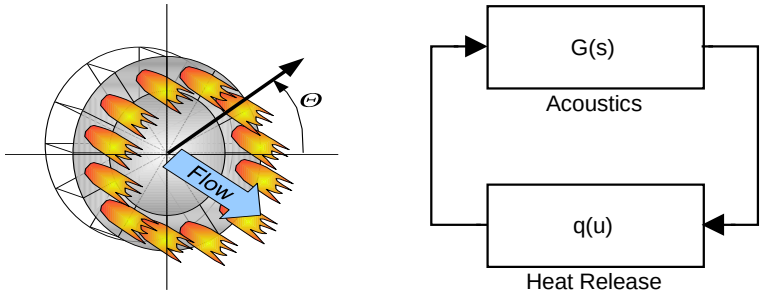

Figure 1: Schematic of the Annular Domain with the First Pair of Fourier Modes

system is available in the works of Culick (i.e. [18]). The transport equations are:

$$\frac{\partial \rho}{\partial t} + \nabla \cdot (u\rho) = 0 \tag{1}$$

$$\rho \frac{\partial u}{\partial t} + \rho u \cdot \nabla u = -\nabla p \tag{2}$$

$$\rho \frac{\partial e}{\partial t} + \rho u \cdot \nabla e = -p \nabla \cdot u + q. \tag{3}$$

where ρ, u, and e are density, velocity, and internal energy per unit volume, p, and q are pressure and a volumetric heat release contribution and the spatial Laplacians describe cylindrical coordinates.

Using a series of assumptions relating to the boundary conditions which can be found in [22] results in a pair of partial differential equations on the annular domain:

$$\frac{\partial u_\Theta}{\partial t} = -a^2 \frac{\partial p}{\partial \Theta} \tag{4}$$

$$\frac{\partial p}{\partial t} + \frac{\partial u_\Theta}{\partial \Theta} = -\zeta p + q, \tag{5}$$

where Θ is the spatial rotational coordinate, ζ is a damping constant, a is the acoustic wavespeed, and q is a driving heat release mechanism.

2.1 Heat Release

The equations (4, 5) are self contained with the exception of the heat release function. The form of the heat release function (q) is the driving component in the feedback loop. Because of the complexity of combustion dynamics, harsh conditions, high noise levels, and lack of adequate sensing apparatus, an analytical form is not yet available. The heat released from combustion is most frequently modeled as a function of acoustic velocity that contains a *saturation like* quality as in [1, 3, 19, 20, 21]. With this in mind we denote the heat release contribution as:

$$q = \sigma[u] + \alpha[u^3] \tag{6}$$

where σ is a linear destabilizing effect, and α is a parameter that introduces the limiting effect ($\alpha < 0$ is chosen).

2.2 Asymmetry Parameter

Prior to discretizing the equations into a modal representation, the acoustic wavespeed is parameterized to have a spatial preference. A perturbation is added to the wavespeed in the form of the second spatial harmonic. The reason for this choice is that using linear analysis in a previous study

[22], it was found that altering the wave-speed in this pattern effected the stability the most. The resulting spatially perturbed acoustic wavespeed is:

$$a = a_0 + \sqrt{2\delta}\cos(2\Theta) \tag{7}$$

where a_0 is a nominal wave-speed and δ is the asymmetry parameter with second harmonic preference.

2.3 Discretization

The discretized equations are obtained by projecting the rotational coordinate onto spatial Fourier modes. The first two spatial modes are retained; $\sin(\Theta), \cos(\Theta)$. A spatio-temporal response in these coordinates is:

$$p(\Theta, t) = \frac{1}{\sqrt{\pi}}\left(p_{sin}(t)\sin(\Theta) + p_{cos}(t)\cos(\Theta)\right) \tag{8}$$

$$u(\Theta, t) = \frac{1}{\sqrt{\pi}}\left(u_{sin}(t)\sin(\Theta) + u_{cos}(t)\cos(\Theta)\right) \tag{9}$$

where p_{sin}, p_{cos} and u_{sin}, u_{cos} are the time dependent modal amplitudes which become the states of our dynamical system. A schematic of these modes on the annular domain is presented in Figure 2.

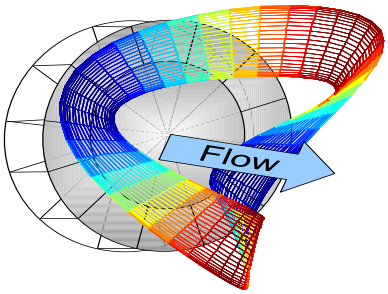

Figure 2: Schematic Representation of the Spectral Modes of the Annular Combustor

The relative amplitude and phase of the temporal coefficients impact the presence of either standing or traveling waves. A standing wave is characterized as a amplitude that depends on position (i.e. a response that has clear nodes and antinodes), while a traveling wave retains a constant amplitude with space. These wave motions have reciprocal relations in that traveling waves can be described using combination of standing waves and vice versa [23]. We are particularly interested in traveling wave solutions and keep in mind that using $\sin(\Theta)$ and $\cos(\Theta)$ as a basis for the dynamics, a traveling wave exists when the amplitudes of the temporal coefficients are equal with a phase difference of $\frac{\pi}{2}$ (and solutions that are trigonometrically symmetric to this).

When using the first two Fourier modes as a basis, the cubic nonlinearity acts through the velocity component and is projected onto the modes as follows:

$$q_{sin} = \frac{\alpha}{\sqrt{\pi}}\int_0^{2\pi} \sin(\Theta)\left(u_{sin}(t)\sin(\Theta) + u_{cos}(t)\cos(\Theta)\right)^3 d\Theta = \alpha\left(\frac{3\sqrt{\pi}}{4}u_{sin}\left(u_{sin}^2 + u_{cos}^2\right)\right) \tag{10}$$

$$q_{cos} = \frac{\alpha}{\sqrt{\pi}}\int_0^{2\pi} \cos(\Theta)\left(u_{sin}(t)\sin(\Theta) + u_{cos}(t)\cos(\Theta)\right)^3 d\Theta = \alpha\left(\frac{3\sqrt{\pi}}{4}u_{cos}\left(u_{sin}^2 + u_{cos}^2\right)\right) \tag{11}$$

and projecting the assumed modal solution onto (4, 5) results in the system of ODE's:

$$\begin{bmatrix} \dot{u}_{sin} \\ \dot{u}_{cos} \\ \dot{p}_{sin} \\ \dot{p}_{cos} \end{bmatrix} = \begin{bmatrix} 0 & 0 & 0 & a_0^2 - \delta \\ 0 & 0 & -a_0^2 - \delta & \\ \sigma & 1 & -\zeta & 0 \\ -1 & \sigma & 0 & -\zeta \end{bmatrix} \begin{bmatrix} u_{sin} \\ u_{cos} \\ p_{sin} \\ p_{cos} \end{bmatrix} + \begin{bmatrix} 0 \\ 0 \\ \alpha\left(\frac{3\sqrt{\pi}}{4}u_{sin}\left(u_{sin}^2 + u_{cos}^2\right)\right) \\ \alpha\left(\frac{3\sqrt{\pi}}{4}u_{cos}\left(u_{sin}^2 + u_{cos}^2\right)\right) \end{bmatrix}$$

To get these equations in the form coupled oscillators, we take $[u_{sin}, u_{cos}]$ as $[x_1, x_2]$ which results in the following second order coupled nonlinear differential equations:

$$x_1'' + \zeta x_1' + (a_0^2 - \delta)x_1 = x_2(a_0^2 - \delta)\left(\sigma - \alpha\left(\frac{3\sqrt{\pi}}{4}\left(x_1^2 + x_2^2\right)\right)\right) \tag{12}$$

$$x_2'' + \zeta x_2' + (a_0^2 + \delta)x_2 = -x_1(a_0^2 + \delta)\left(\sigma + \alpha\left(\frac{3\sqrt{\pi}}{4}\left(x_1^2 + x_2^2\right)\right)\right) \tag{13}$$

From this representation, the architecture of the system becomes clear. Once projected onto the two modes, the dynamics are two stable oscillators with skew symmetric coupling due to the heat release.

For the remainder of this study, we will investigate the behavior of system (12, 13) specifically focusing on two parameters; σ which is the skew symmetric coupling parameter from heat release, and δ which is the asymmetry parameter. We begin by studying behavior of the global equilibrium and continue by investigating the periodic equilibria and their stability. For the analysis to follow, we will use the values in Table 1 as a set of *nominal* parameters.

Table 1: Nominal Parameters

a_0	ζ	σ	α	δ
1.0	0.2	0.5	-0.0018	0.0

3 Equilibrium Analysis

The system (12, 13) contains one equilibrium point at the origin, and in this section we investigate the stability of this equilibrium with respect to both the linear coupling parameter, and the asymmetry parameter. When the asymmetry parameter (δ) and coupling term (σ) are zero, evaluation of the Jacobian at the origin reveals a set of co-located stable eigenvalue pairs at $\frac{1}{2}\left(-\zeta \pm \sqrt{-4a_0^2 + \xi_0^2}\right)$.

When the coupling is increased from zero these complex eigenvalues become:

$$\begin{aligned} \lambda_{1,2} &= \frac{-\zeta - \sqrt{\zeta^2 - 4a_0^2 \pm 4\sqrt{-\sigma^2 a_0^4}}}{2} \\ \lambda_{3,4} &= \frac{-\zeta + \sqrt{\zeta^2 - 4a_0^2 \pm 4\sqrt{-\sigma^2 a_0^4}}}{2} \end{aligned} \tag{14}$$

It is evident that with sufficiently large values of positive or negative coupling the eigenvalues break apart, moving left and right in the complex plane. Physically, the case with $\sigma = 0$ represents zero combustion (the eigenvalues are purely acoustic), and the case with nonzero σ portrays the case with the driving combustion process. With sufficient heat addition, one pair of complex eigenvalues eventually crosses the imaginary axis. The value of the coupling parameter such that the eigenvalues cross the imaginary axis is:

$$\sigma_{crit} = \frac{\zeta}{a_0} \tag{15}$$

From this we see that instability occurs when the coupling from positive feedback exceeds the acoustic damping normalized by the nominal wavespeed. When the coupling from heat release is further increased the eigenvalues continue to become more unstable, the oscillations grow and are eventually limited by nonlinearity. Figure 3 shows results from the numerical bifurcation analysis tool AUTO illustrating the Hopf Bifurcation leading to instability without any modification of symmetry (the *system parameter* is oscillation amplitude).

The stabilizing effect of adding asymmetry to the combustion dynamics is performed by investigating the behavior of the system under variations of the asymmetry parameter δ. Taking a nonzero positive value for σ which insures oscillations in the dynamics, we perform eigenvalue analysis in a

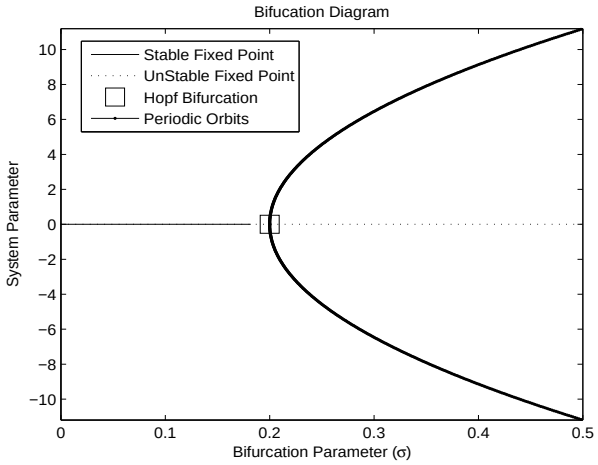

Figure 3: Bifurcation Solutions Representing the Destabilizing Effect of the Parameter σ

similar way. The results show that increasing asymmetry provides a stabilizing mechanism, and the critical value that returns the eigenvalues to the stable half of the complex plane is:

$$\delta_{crit}^2 = \frac{a_0\sqrt{a_0^2\sigma^2 - \zeta^2}}{\sqrt{1+\sigma^2}} \tag{16}$$

Similar numerical bifurcation results of the system with its symmetry altered showing its stabilizing effect (Figure 4).

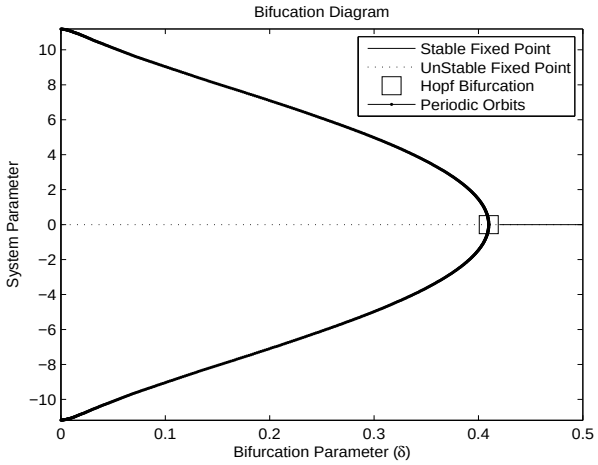

Figure 4: Bifurcation Solutions Representing the Stabilizing Effect of the Parameter δ

The focus of this study is to generate both analytical and numerical results which are similar to the schematics of Figures 3 and 4. Specifically, we investigate the amplitude and stability of the limit cycle when $\sigma > \sigma_{crit}$ and $0 < \delta < \delta_{crit}$.

4 Periodic Solutions

To analyze the bifurcation branches and periodic behavior of the combustion system, we rely on the characteristic that the dynamics are nearly linear. The linearity of the system is addressed by rearranging the terms of the nonlinear system (12, 13) into a standard oscillator form and entering in the nominal parameters. The equations become:

$$\begin{aligned} x_1'' + x_1 &= -0.2x_1' + \delta x_1 + 0.5(-\delta + 1)x_2 + 0.0024(\delta - 1)x_1^2 x_2 + 0.0024(\delta - 1)x_2^3 \\ x_2'' + x_2 &= -0.2x_2' - \delta x_2 + 0.5(-\delta - 1)x_1 + 0.0024(\delta + 1)x_1 x_2^2 + 0.0024(\delta + 1)x_1^3 \end{aligned} \tag{17}$$

With small variation in the asymmetry parameter δ the system remains *closely linear* in its behavior. This is also confirmed by the mostly sinusoidal response of equations from time integration (i.e. simulation with an ODE solver). Another point of interest which is evident in (17) is that the terms on the right hand side consist of driving from heat addition and dissipation from damping in the acoustics. It is a balance of these two mechanisms that is the manifestation of the periodic response of the system.

Since the dynamics of the system appear to first order as those of a linear oscillator with small perturbation, we have a few options for approximate analysis of the dynamics. Below we present two approaches averaging (in two different coordinate systems), and harmonic balance to obtain the *slow flow* dynamics of the trajectories.

4.1 Averaging

The first approach to obtain the slow flow of equations (12, 13) includes the use of time averaging (see [24]). We perform this approximation using two different basis, polar coordinates, and using action angle variables. We show that the averaged results are identical using either approach.

The averaging approach includes making a harmonic assumption of the limit cycle response exploiting a time scale assumption on the assumed solution (i.e. variation of parameters), and integration in time (averaging). What results is the slow flow (ie amplitude and phase ODE's). We we will investigate the equilibria of this reduced system both with and without assymetry.

4.1.1 Averaging in Polar Coordinates

We begin by making the assumption that the response is harmonic with slowly varying amplitude and phase parameters:

$$x_i(t) = R_i(t)Cos(\omega t + \phi_i(t)) \tag{18}$$

where i relates to the two oscillators describing the amplitudes of the sine and cosine acoustic modes. For this study, we are concerned with solutions where the period of each oscillation is equal and stationary. Differentiation in time results in:

$$x'(t) = -\omega R_i(t)Sin(\omega t + \phi_i(t)) - \phi_i'(t)R_i(t)Sin(\omega t + \phi_i(t)) + R_i'(t)\cos(\omega t + \phi_i(t)) \tag{19}$$

where $(.)'$ represents differentiation with respect to time. The assumption that the amplitude and phase of the assumed solution vary slowly with time reveals that their time derivative has negligible contribution to the velocity states which is equivalent to solution of the ODE using *variation of parameters*[26]. With this in mind, we assume :

$$0 = -\phi_i'(t)R_i(t)\sin(\omega t + \phi_i(t)) + R_i'(t)\cos(\omega t + \phi_i(t)) \tag{20}$$

which results in the velocity state as:

$$x'(t) = -\omega R_i(t)\sin(\omega t + \phi_i(t)) \tag{21}$$

The assumed solutions (18), and (21), and the time derivative of (21) are substituted into the equations of motion. Using this equation and (20) results in two equations and two unknowns for each

oscillator. Isolating the time derivatives of the unknowns $(R_i'(t), \phi_i'(t))$ results in an ODE describing the slow evolution of the amplitude and phase of the limit cycle. This differential equation system will contain the parameters of the system $(\sigma, \alpha, a_0, \xi_0)$ the states of the slow flow $(R_i(t), \phi_i(t))$, and resonant terms (i.e. $\cos(\omega t), \sin(\omega t)$). The next step is to remove the resonant terms by averaging over one period of oscillation. Before doing this we change the coordinates to consider relative phase variables:

$$\begin{array}{ll} \psi_+ = \frac{1}{2}\left(\theta_1 + \theta_2\right), & \psi_- = \theta_1 - \theta_2 \\ \text{or } \theta_1 = \frac{\psi_-}{2} + \psi_+, & \theta_2 = \psi_+ - \frac{\psi_-}{2} \end{array} \tag{22}$$

and perform the averaging:

$$\frac{d\overline{R}_i}{dt} = \frac{1}{T}\int_0^T f(R, \psi, t)dt \tag{23}$$

$$\frac{d\overline{\psi}_i}{dt} = \frac{1}{T}\int_0^T f(R, \psi, t)dt \tag{24}$$

where $T = \frac{2\pi}{\omega}$, and the function $f(R, \psi, t)$ contains information from both oscillators due to the coupling, and the overbar denotes averaged quantities. The resulting system is:

$$\begin{aligned} \bar{\psi}_+' &= \frac{\cos\left(\bar{\psi}_-\right)\left(16\sigma + 9\sqrt{\pi}\alpha\left(\bar{R}_1^2 + \bar{R}_2^2\right)\right)\left(\left(\bar{R}_1 - \bar{R}_2\right)\left(\bar{R}_1 + \bar{R}_2\right)a_0^2 + \delta\left(\bar{R}_1^2 + \bar{R}_2^2\right)\right)}{64 a_0 \bar{R}_1 \bar{R}_2} \\ \bar{\psi}_-' &= -\frac{32\delta\bar{R}_1\bar{R}_2 + \cos\left(\bar{\psi}_-\right)\left(\left(a_0^2 + \delta\right)\bar{R}_1^2 + \left(a_0^2 - \delta\right)\bar{R}_2^2\right)\left(16\sigma + 9\sqrt{\pi}\alpha\left(\bar{R}_1^2 + \bar{R}_2^2\right)\right)}{32 a_0 \bar{R}_1 \bar{R}_2} \\ \bar{R}_1' &= -\frac{16\zeta a_0 \bar{R}_1 + \sin\left(\bar{\psi}_-\right)\left(a_0^2 - \delta\right)\bar{R}_2\left(16\sigma + 3\sqrt{\pi}\alpha\left(\bar{R}_1^2 + 3\bar{R}_2^2\right)\right)}{32 a_0} \\ \bar{R}_2' &= -\frac{16\zeta a_0 \bar{R}_2 + \sin\left(\bar{\psi}_-\right)\left(a_0^2 + \delta\right)\bar{R}_1\left(16\sigma + 3\sqrt{\pi}\alpha\left(3\bar{R}_1^2 + \bar{R}_2^2\right)\right)}{32 a_0} \end{aligned} \tag{25}$$

Studying the equilibrium points of (25) reveals the amplitude and phase of the limit cycle when the limit cycle in the system exists due to sufficient heat release (i.e. $\sigma > \sigma_{crit}$). We will study these equilibria and how they are effected by assymmetry in Section 5.

4.1.2 Averaging in Action Angle Coordinates

To perform the averaging in action angle coordinates, we first define the canonical transformation:

$$x_1(t) = \sqrt{2J_1(t)}\cos\left(\theta_1(t)\right), \quad x_1(t)' = \sqrt{2J_1(t)}\sin\left(\theta_1(t)\right) \tag{26}$$

$$x_2(t) = \sqrt{2J_2(t)}\cos\left(\theta_2(t)\right), \quad x_2(t)' = \sqrt{2J_2(t)}\sin\left(\theta_2(t)\right) \tag{27}$$

where again as designated, the action and angle variables are functions of time. The second derivative in time is found from differentiation of the above relations (i.e. $x_1'' = \frac{d(x_1')}{dt}$) and after substituting the coordinate transforms, we have two equations and four differential variables $(J_1, J_2, \theta_1, \theta_2)$. Two additional equations are realized by the constraint equations (again from variation of parameters):

$$\frac{dx_1}{dt} = x_1', \quad \frac{dx_2}{dt} = x_2' \tag{28}$$

for nature of the assumed quantities in 26, and 27.

After these substitutions, we can solve for the differential variables of the system $(J_1', J_2', \theta_1', \theta_2')$ resulting in a fourth order ordinary differential equation system. Again, we transform the phase variables to the form in Equation 22 resulting in a differential equation system $(J_1', J_2', \psi_+', \psi_-')$. In this coordinate system, the phase variable ψ_+ acts like time and hence we average the dynamics over this variable:

$$\bar{f} = \frac{1}{2\pi}\int_0^{2\pi} f d\psi_+ \tag{29}$$

The averaged system in Action Angle coordinates is then:

$$\begin{aligned}
\bar{\psi}'_{+} &= -\frac{16\sqrt{\bar{J}_1}\sqrt{\bar{J}_2}\left(a_0^2+1\right)+\cos\left(\bar{\psi}_-\right)\left(8\sigma+9\sqrt{\pi}\alpha\left(\bar{J}_1+\bar{J}_2\right)\right)\left(\left(\bar{J}_1-\bar{J}_2\right)a_0^2+\delta\left(\bar{J}_1+\bar{J}_2\right)\right)}{32\sqrt{\bar{J}_1}\sqrt{\bar{J}_2}} \\
\bar{\psi}'_{-} &= \delta+\frac{\cos\left(\bar{\psi}_-\right)\left(8\sigma+9\sqrt{\pi}\alpha\left(\bar{J}_1+\bar{J}_2\right)\right)\left(\left(\bar{J}_1+\bar{J}_2\right)a_0^2+\delta\left(\bar{J}_1-\bar{J}_2\right)\right)}{16\sqrt{\bar{J}_1}\sqrt{\bar{J}_2}} \\
\bar{J}'_1 &= \tfrac{1}{8}\sqrt{\bar{J}_1}\left(\sin\left(\bar{\psi}_-\right)\left(a_0^2-\delta\right)\sqrt{\bar{J}_2}\left(8\sigma+3\sqrt{\pi}\alpha\left(\bar{J}_1+3\bar{J}_2\right)\right)-8\zeta\sqrt{\bar{J}_1}\right) \\
\bar{J}'_2 &= \tfrac{1}{8}\sqrt{\bar{J}_2}\left(\sin\left(\bar{\psi}_-\right)\left(a_0^2+\delta\right)\sqrt{\bar{J}_1}\left(8\sigma+3\sqrt{\pi}\alpha\left(3\bar{J}_1+\bar{J}_2\right)\right)-8\zeta\sqrt{\bar{J}_2}\right)
\end{aligned} \tag{30}$$

4.2 Harmonic Balance

The variable coefficient harmonic balance method provides another approximation to the limit cycle dynamics and to develop it we begin with the assumed harmonic solution (18), differentiate as necessary and insert into the equations of motion (12, 13). Similar to the use of *variation of parameters*, the coefficients of the assumed harmonic solution are considered slowly varying. Because of this, as in [25], the second order derivatives of the amplitude and phase coefficients of the assumed solution are considered negligible. By collecting the sine and cosine terms of each equation (the coefficients of the resonant terms) we obtain two differential equations for each oscillator. Similar to the slow flow system derived from Averaging this ODE describes the slow evolution of amplitude and phase of the assumed solution. We may again solve for the time derivatives of the unknown coefficients, and the equilibriums will describe the limit cycle conditions.

If we consider the resonant case, the period of oscillation will be related to the wavespeed and therefore the natural frequency of the assumed solution will equal the wave speed ($\omega = a_0$). After including this into the equations of motion, we have the slow flow system:

$$\begin{aligned}
R'_1 &= \frac{3\sqrt{\pi}\alpha(3\mathrm{k}2\zeta+2\mathrm{k}1a_0)\left(a_0^2-\delta\right)R_2R_1^2+16\zeta\left(\delta-2a_0^2\right)R_1+(\mathrm{k}2\zeta+2\mathrm{k}1a_0)\left(a_0^2-\delta\right)R_2\left(9\sqrt{\pi}\alpha R_2^2+16\sigma\right)}{16\left(\zeta^2+4a_0^2\right)} \\
R'_2 &= -\frac{-3\sqrt{\pi}\alpha(2\mathrm{k}1a_0-3\mathrm{k}2\zeta)\left(a_0^2+\delta\right)R_1R_2^2+16\zeta\left(2a_0^2+\delta\right)R_2-(2\mathrm{k}1a_0-\mathrm{k}2\zeta)\left(a_0^2+\delta\right)R_1\left(9\sqrt{\pi}\alpha R_1^2+16\sigma\right)}{16\left(\zeta^2+4a_0^2\right)} \\
\psi'_{-} &= \frac{9\sqrt{\pi}\alpha(\mathrm{k}1\zeta+2\mathrm{k}2a_0)\left(a_0^2+\delta\right)R_1^4+2\left(3\sqrt{\pi}\alpha\left(6\mathrm{k}2a_0^3+\mathrm{k}1\delta\zeta\right)R_2^2+8\sigma(\mathrm{k}1\zeta+2\mathrm{k}2a_0)\left(a_0^2+\delta\right)\right)R_1^2}{16\left(\zeta^2+4a_0^2\right)R_1R_2}+\cdots \\
&\quad+\frac{64\delta a_0R_2R_1+(2\mathrm{k}2a_0-\mathrm{k}1\zeta)\left(a_0^2-\delta\right)R_2^2\left(9\sqrt{\pi}\alpha R_2^2+16\sigma\right)}{16\left(\zeta^2+4a_0^2\right)R_1R_2} \\
\psi'_{+} &= \frac{-9\sqrt{\pi}\alpha(\mathrm{k}1\zeta+2\mathrm{k}2a_0)\left(a_0^2+\delta\right)R_1^4-2\left(3\sqrt{\pi}\alpha a_0(6\mathrm{k}2\delta+\mathrm{k}1\zeta a_0)R_2^2+8\sigma(\mathrm{k}1\zeta+2\mathrm{k}2a_0)\left(a_0^2+\delta\right)\right)R_1^2}{32\left(\zeta^2+4a_0^2\right)R_1R_2}+\cdots \\
&\quad+\frac{32\zeta^2a_0R_2R_1+(2\mathrm{k}2a_0-\mathrm{k}1\zeta)\left(a_0^2-\delta\right)R_2^2\left(9\sqrt{\pi}\alpha R_2^2+16\sigma\right)}{32\left(\zeta^2+4a_0^2\right)R_1R_2}
\end{aligned} \tag{31}$$

where $k1 = \sin\psi_-$ and $k2 = \cos\psi_-$.

5 Comparison of Methods and Numerical Results

In this section we compare the results of the different approximation methods. We first present the dynamics when the asymmetry parameter is set to zero (the value of the equilibria, and the associated phase space of the reduced system). A comparison is also presented for the amplitudes of the limit cycle with varying asymmetry. It is shown that the three different approximations to the full nonlinear system are in agreement with each other and that the asymmetry parameter always reduces the amplitude of the limit cycle.

5.1 Reduced Phase Space Comparison

When the asymmetry parameter is set to zero the dynamics are symmetric and therefore the amplitude of the two acoustic modes are identical. This offers a means to investigate the system on a two dimensional plane.

For the case with averaging in polar coordinates, we let $\bar{R}_1 = \bar{R}_2 = \bar{R}$ and $\delta = 0$ in Equation (25) and obtain the reduced system:

$$\begin{aligned} \bar{\psi}'_+ &= 0 \\ \bar{\psi}'_- &= -\tfrac{1}{16}\cos\left(\bar{\psi}_-\right)\left(18\sqrt{\pi}\alpha\bar{R}^2 + 16\sigma\right)a_0 \\ \bar{R}' &= -\tfrac{\bar{R}\left(12\sqrt{\pi}\alpha\bar{R}^2+16\sigma\right)\sin\left(\bar{\psi}_-\right)a_0^2+16\zeta\bar{R}a_0}{32a_0} \end{aligned} \tag{32}$$

The equilibrium points of 32 are found by setting time derivatives to zero. The nontrivial real solutions are presented in Table 2, with the numerical substitution using the nominal parameters.

In the approximation using averaging in action angle coordinates we investigate the nominal symmetric case by letting $\bar{J}_1 = \bar{J}_2 = \bar{J}$, $\delta = 0$ in the differential equation system (30). The resulting equations are:

$$\begin{aligned} \bar{\psi}'_+ &= \tfrac{1}{2}\left(-a_0^2 - 1\right) \\ \bar{\psi}'_- &= \tfrac{1}{8}\cos\left(\bar{\psi}_-\right)\left(8\sigma + 18\sqrt{\pi}\alpha\bar{J}\right)a_0^2 \\ \bar{J}' &= \tfrac{1}{8}\sqrt{\bar{J}}\left(\sqrt{\bar{J}}\left(8\sigma + 12\sqrt{\pi}\alpha\bar{J}\right)\sin\left(\bar{\psi}_-\right)a_0^2 - 8\zeta\sqrt{\bar{J}}\right) \end{aligned} \tag{33}$$

The equilibrium points of 33 are presented in Table 2. Note that the conversion of $R \approx \sqrt{2J}$ provides exact agreement in these results between averaging in polar and action angle coordinates (and the harmonic balance for that matter).

For the case where Harmonic Balance is utilized as an approximation, we investigate the symmetric case by letting $R_1 = R_2 = R$ and $\delta = 0$ resulting in:

$$\begin{aligned} R'(t) &= \tfrac{Ra_0^2\left(\left(9\sqrt{\pi}\alpha R^2+8\sigma\right)\cos(\psi_-)\zeta-16\zeta+4\left(3\sqrt{\pi}\alpha R^2+4\sigma\right)\sin(\psi_-)a_0\right)}{8\left(\zeta^2+4a_0^2\right)} \\ R'(t) &= \tfrac{Ra_0^2\left(4\left(3\sqrt{\pi}\alpha R^2+4\sigma\right)\sin(\psi_-)a_0-\zeta\left(\left(9\sqrt{\pi}\alpha R^2+8\sigma\right)\cos(\psi_-)+16\right)\right)}{8\left(\zeta^2+4a_0^2\right)} \\ \psi'_- &= \tfrac{\left(9\sqrt{\pi}\alpha R^2+8\sigma\right)\cos(\psi_-)a_0^3}{2\left(\zeta^2+4a_0^2\right)} \\ \psi'_+ &= \tfrac{\zeta a_0\left(4\zeta-\left(3\sqrt{\pi}\alpha R^2+4\sigma\right)\sin(\psi_-)a_0\right)}{4\left(\zeta^2+4a_0^2\right)} \end{aligned} \tag{34}$$

In this system, the term ψ_+ is a decoupled non-equilibrium state that acts similar to time. Therefore we omit this differential equation and perform the steady state analysis. The nontrivial real equilibria of the symmetric system are presented in Table 2.

Table 2: Equilibria for the Symmetric Case (Comparison of Different Methods)

-	Averaging (Polar)	Averaging (Action-Angle)	Harmonic Balance
Amplitude	$\bar{R} = \frac{2\sqrt{\pm\zeta-\sigma a_0}}{\pi^{\frac{1}{4}}\sqrt{3\alpha a_0}}$ $= \{17.10, 11.19\}$	$\bar{J} = \pm\frac{2\left(\zeta\mp\sigma a_0^2\right)}{3\sqrt{\pi}\alpha a_0^2}$ $= \{62.68, 146.27\}$	$R = \frac{2\sqrt{\pm\zeta-\sigma a_0}}{\pi^{\frac{1}{4}}\sqrt{3\alpha a_0}}$ $= \{17.10, 11.19\}$
Phase	$\bar{\psi}_- = \pm\frac{\pi}{2}, \pm\frac{\pi}{2}$	$\bar{\psi}_- = \pm\frac{\pi}{2}, \pm\frac{\pi}{2}$	$\bar{\psi}_- = \pm\frac{\pi}{2}, \pm\frac{\pi}{2}$

As seen in the table there is agreement between all three approximate methods. Additionally, since the system has been reduced to a second order system, we can investigate its phase space graphically. The phase space of the averaged system (32) is presented in Figure 5 (the phase space for all three methods is indistinguishable graphically, so for brevity we present the vector field from averaging in polar coordinates). From this, we find that the equilibrium point $\bar{R} = 11.19$, $\bar{\psi}_- = -\frac{\pi}{2}$ is stable, while all other equilibria are unstable, which was confirmed by evaluation of the Jacobian at these equilibria.

5.2 Amplitude Comparisons

Now that we are familiar with the approximate system when the asymmetry parameter is zero, we investigate the response of the limit cycle amplitude when the symmetry of the acoustic wavespeed

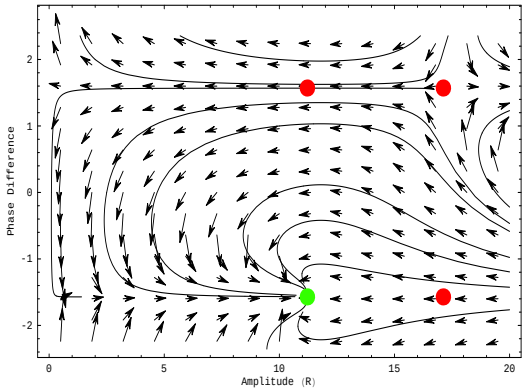

Figure 5: Phase Space of the Nominally Symmetric System Reduced to a 2D Field

is modified on the annular domain. In this section we provide a comparison of oscillator amplitude (12, 13) using three different methods including averaging in polar and action angle coordinates, as well as the harmonic balance with nonzero asymmetry. In each case, fixed points of the ordinary differential equations were found by time integration of the system of equations, retaining the final point when the dynamics have settled. In all cases, the nominal system parameters are those described in Section 2, while the symmetry parameter is varied as the independent variable. Figure 6 illustrates the amplitude of the limit cycle for each acoustic mode (each oscillator in (12, 13)).

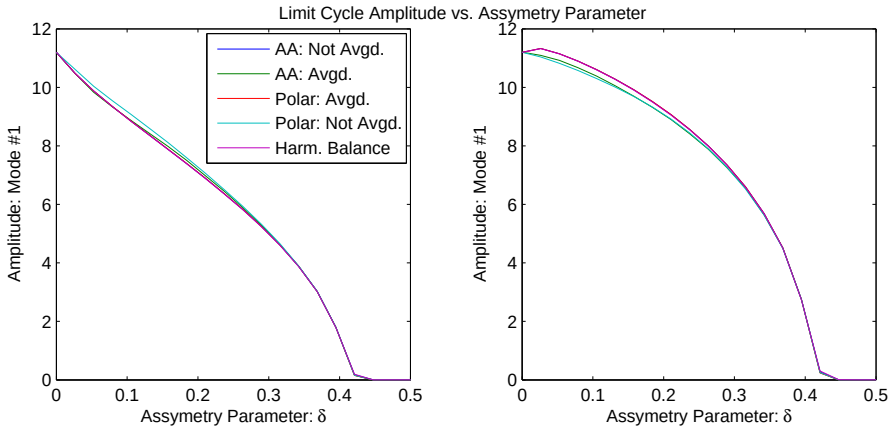

Figure 6: Mode Amplitudes as a function of the Asymmetry Parameter (the Action Angle Results are scaled)

In this figure, the influence of the asymmetry parameter (δ) presents an attenuating influence on the amplitudes of the oscillations ultimately quenching the response. In addition, we notice that these amplitudes decrease at different rates which occurs because when altering the symmetry of the system, the dynamics prefer one spatial mode over the other, and the corresponding state variable behaves accordingly. It is also clear that the solutions agree quiet well between the original and approximate dynamics.

The above plots trace the stable solutions of the system in both its full and approximate state. We are also interested in the effect of asymmetry on the unstable solutions. Below, in Figure 7 trace both the stable and unstable branches as the asymmetry is increased. For this we simply use a gradient search on the right hand sides of the approximate differential equations (seeking zero).

This figures shows that when $\delta = 0$ and $R_1 = R_2$ there exists two values (11.19,17.10) corresponding to the stable and unstable equilibria. With an increase in δ the stable solution begins to

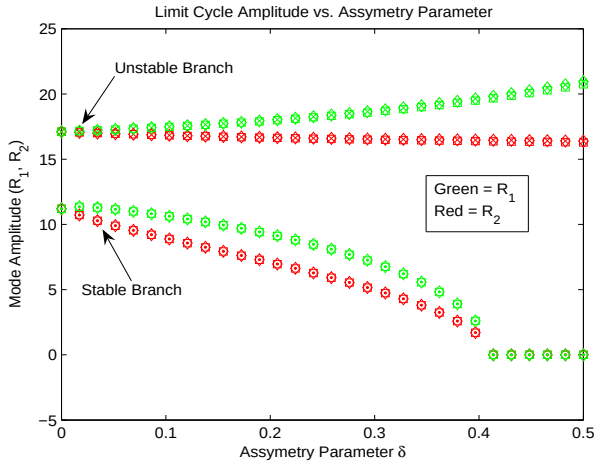

Figure 7: Mode Amplitudes as a function of the Asymmetry Parameter for Three Different Approximations (note all approximations are nearly equivalent, and the Action Angle Results are scaled)

decrease in amplitude (R_1 and R_2 at different rates) and eventually reaches zero. For the unstable solution which starts at 17.10 increasing δ also effects the amplitudes (at different rates) but it is evident that these solutions do not interact with the stable branch.

5.3 Orbit Stability

As we have shown, symmetry effects amplitudes while to be sufficiently applicable for engineering application, these new orbits must be stable to account for unmodeled characteristics or external influences. Therefore, it is necessary to assess the stability of the periodic solutions of this system under influence of the asymmetry to characterize the robustness of the use symmetry in the system to reduce oscillation amplitudes. To perform this analysis, the slow flow equations developed from the averaging method in action angle coordinates (30) are linearized about the stable equilibria in Figure 7. The eigenvalues of these fixed points is presented in Figure 8.

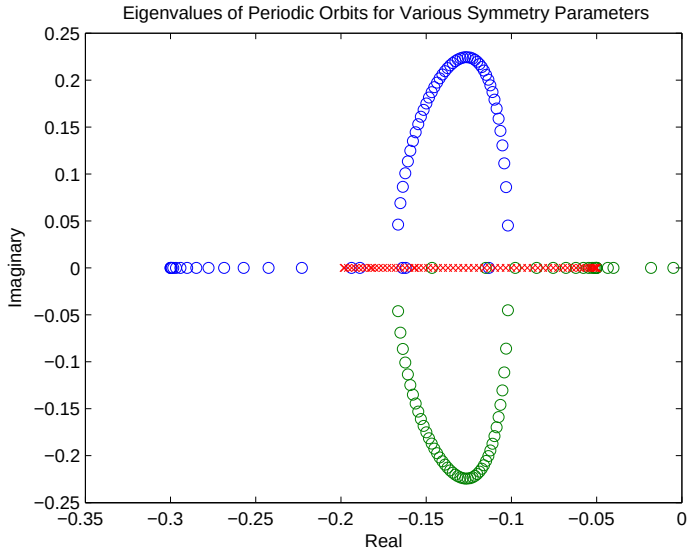

Figure 8: Eigenvalues of the Periodic Orbits with the influence of Asymmetry

The figure above illustrates that the orbits remain stable under all conditions where the slow flow equations are valid. The behavior of these dynamics are such that all solutions are stable and real when the symmetry parameter is set to zero. Upon increasing this parameter, two eigenvalues break apart and become complex pairs. Clearly these eigenvalues are associated with the amplitude evolution dynamics (as verified by investigating the eigenvectors), while the third eigenvalue remains real and is associated with the differential phase between the two oscillator dynamics. This particular eigenvalue approaches instability as the amplitude equilibrium approaches zero but remains stable.

6 Summary

In this paper we have modeled thermoacoustic dynamics in an annular combustor and reduced these dynamics to a coupled oscillator system including a parameter for the spatial symmetry of the passive dynamics. We have shown that the nonlinear coupling due to heat release, always imposes an adverse effect on the system, resulting in a limit cycle exhibited by a traveling acoustic wave. We have also shown that spatial perturbation in the symmetry of the acoustic wavespeed reduces the amplitude of the limit cycle (in a stable way) eventually stabilizing the system. These results have been concluded using three different nonlinear analysis tools.

Acknowledgements

This work was supported by AFOSR contract F49620-01-C-0021, which is gratefully acknowledged. The authors would also like to thank, Dr. Prashant Mehta (University of Illinois, Urbana-Champaign), Dr. Umesh Vaidya (Iowa State University), and Dr. Tamás Kalmár-Nagy (Texas A&M) for many fruitful discussions.

References

[1] A. P. Dowling. Nonlinear self-excited oscillations of a ducted flame. *Journal of Fluid Mechanics*, 346:271–290, 1997.

[2] M. Fleifil, A. M. Annaswamy, Z. A. Ghoneim, and A. F. Ghoniem. Response of a laminar premixed flame to flow oscillations: A kinematic modal and thermoacoustic instability results. *Combustion and Flame*, 106:487–510, 1996.

[3] A. Peracchio and W. Proscia. Nonlinear heat release/acoustic model for thermo-acoustic instability in lean premixed combustors. *ASME paper 98-GT-269*, 1998.

[4] C. A. Jacobson, A. I. Khibnik, A. Banaszuk, J. Cohen, and W. Proscia. Active control of combustion instabilities in gas turbine engines for low emissions. part 1: Phisycs-based and experimentally identified models of combustion instability. *Applied Vehicle Technology Panel Symposium on Active Control Technology, Brauschweig, Germany*, 2000.

[5] S. Stow and A. Dowling. Thermoacoustic oscillations in an annular combustor. *Proceedings of the ASME Turbo Expo, ASME paper 2001-GT-0037*, 2001.

[6] S. Stow and A. Dowling. Modelling of circumferential modal coupling due to helmoltz resonators. *Proceedings of the ASME Turbo Expo, ASME paper 2003-GT-38168*, 2003.

[7] S. Stow and A. Dowling. Low-order modelling of thermoacoustic limit cycles. *Proceedings of the ASME Turbo Expo, ASME paper GT2004-54245*, 2004.

[8] K. Kunze, C Hirsch, and T. Sattelmayer, "Thermoacoustic modeling and control of multi burner combustion systems" *Proceedings of the ASME Turbo Expo, ASME paper 2003-GT-38688*, 2003.

[9] W. Krebs, G. Walz, and S. Hoffmann. Thermoacoustic analysis of annular combustor. *AIAA Paper 99-1971*, 1999.

[10] S. M. Candel. Combustion instabilities coupled by pressure waves and their active control. *Fourth International Symposium on Combustion, The Combustion Institute*, pages 1277–1296, 1992.

[11] C.O. Paschereit and E. Gutmark. The effectiveness of passive combustion control methods. *Proceedings of the ASME Turbo Expo, Vienna, Austria*, 2004.

[12] A. Banaszuk, G. Hagen, P. Mehta, and J. Oppelstrup. A linear model for control of thermoacoustic instabilities on an annular domain. *Proceedings of the IEEE Conference on Decision and Control*, 2003.

[13] M. Krstic and A. Banaszuk. Multivariable adaptive control of instabilities arising in jet engines. *Submitted to Journal of Control Engineering Practice*, 2005.

[14] B. Schuermans, V. Bellucci, and C.O. Paschereit. Thermoacoustic modeling and control of multi burner combustion systems. *Proceedings of the ASME Turbo Expo, Atlanta, Georgia*, 2003.

[15] J.T. Ariaratnam, S.H. Strogatz, "Phase diagram for the Winfree model of coupled nonlinear oscillators", *Phys. Rev. Lett.* 86 (2001) 4278–4281.

[16] P.C. Bressloff and S. Coombes "Traveling Waves in a Chain of Pulse-Coupled Oscillators" *Physical Review Letters* Vol 80, Number 21, 25 May 1998.

[17] Barahona, M. and Pecora, L. M., "Synchronization in small-world systems", *Phys. Rev. Lett.* 89, 054101 (2002).

[18] F.E.C. Culick, "A note on Rayleigh's Criterion" *Combustion Science, and Technology* Vol 56, pp. 159-166 1987.

[19] R. Balachandran and B.O. Ayoola and C.F. Kaminski and A.P. Dowling and E. Mastorakos, "Experimental Investigation of the nonlinear Response of turbulent Premixed Flames to imposed inlet velocity Oscillations" *Combustion and Flame* Vol. 143. 2005.

[20] T. Lieuwen and Y. Neumeier, "Nonlinear Pressure-Heat Release Transfer Function Measurements in a premixed combustor" *Proceedings of the Combustion Institute* Vol. 29. 2002.

[21] T. Lieuwen and B. Bellows, "Nonlinear Kinematic Response of Premixed Flames to Harmonic Velocity Disturbances" *Proceedings of the Third Joint Meeting of the U.S. Sections of the Combustion Institute* 2002.

[22] G. Hagen and A. Banaszuk, "Uncertainty Propagation in a Reduced Order Thermo-acoustic Model" 43rd IEEE Conference onf Decision and Control, 2004.

[23] L.E. Kinsler, A.R. Frey, et.al *Fundamentals of Acoustics, Third Edition* John Wiley and Sons, 1982.

[24] J. Guckenheimer and P. J. Holmes, *Nonlinear Oscillations, Dynamical Systems and Bifurcations of Vector Fields* Springer, New York 1983.

[25] B. Van Der Pol, "Forced Oscillations in a Circuit with non-linear Resistance" *Phil. Mag.* S. 7. Vol. 3. No. 13. 1927.

[26] W.I. Newman, M. Efroimsky, "The Method of Variation of Constants and Multiple Time Scales in Orbital Mechanics" 34th Meeting of the AAS Division on Dynamical Astronomy, May 2003.